Journal of Experimental Psychology:
Human Perception and Performance
1991, Vol. 17, No. 3, 635-651


0096-1523/91/$3.00

# Dynamical Substructure of Coordinated Rhythmic Movements

R. C. Schmidt
Center for the Ecological Study of Perception and Action
University of Connecticut

P. J. Beek
Center for the Ecological Study of Perception and Action
University of Connecticut
Free University, Amsterdam, The Netherlands

P. J. Treffner
Center for the Ecological Study of Perception and Action
University of Connecticut

M. T. Turvey
Center for the Ecological Study of Perception and Action
University of Connecticut
Haskins Laboratories, New Haven, Connecticut

A coordinated rhythmic movement pattern is a dynamical activity involving many hidden layers of rhythmic subtasks. To investigate this dynamical substructure, spectroscopic concepts and methods were applied to an interlimb rhythmic movement task requiring 1:1 frequency locking of two hand-held pendulums in 180° phase relation. The pendulums could be of identical or very different dimensions, thereby providing different values of the ratio Ω of uncoupled frequencies. Analyses focused on the power spectrum of continuous relative phase as a function of variation in Ω. Predictions were derived from the theories of mode locking and fractal time. Experimental results were in agreement with theoretical expectations and were discussed in terms of the possible recruiting of rhythmic subtasks in the assembling of interlimb absolute coordination, the interdependence of these subtasks, and the general dynamical principles that relate coordinative processes occurring at different length and time scales.

The most common form of interlimb coordination is that in which two or more limbs or limb segments oscillate at the same frequency. Von Holst (1939/1973) referred to this type of coordination as *absolute coordination*. Casual observation suggests that a person can achieve 1:1 frequency locking with any two biokinematic links regardless of the size difference and, therefore, the inertial difference, between them. Thus, rhythmic motions of the two hands, or of the two legs, can be conducted at a common tempo, but so can rhythmic motions of the head and a foot, of a leg and a little finger, of a hand and a forearm, and so on. Given that inertial differences can be shown to translate into differences in preferred (uncoupled) frequencies (Kugler & Turvey, 1987; Turvey, Schmidt, Rosenblum, & Kugler, 1988), it appears that 1:1 frequency locking is achievable over wide variation in the frequency ratio Ω of the (uncoupled) biokinematic links.

In this article we present an experimental analysis of this ability to achieve isochrony of body segments. Data are reported on the 1:1 frequency locking of rhythmic movement units with identical or different frequencies. The experimental rhythmic movement unit is defined by a hand-held pendulum and the neuromuscular processes by which the pendulum is moved rhythmically around an axis in the wrist (Kugler & Turvey, 1987). The characteristic frequency of such a rhythmic unit—a wrist–pendulum system—is determined primarily by the pendulum's length. To study 1:1 frequency locking, the subject is given a pendulum to hold and swing in each hand; the two pendulums can be of the same size (same characteristic frequency) or of different sizes (different characteristic frequencies). Varying the length of the pendulum held in the right hand in relation to the length of that held in the left hand is a convenient way to vary Ω. Kugler and Turvey (1987) showed that subjects can achieve 1:1 frequency locking in this inter–wrist–pendulum coordination task over wide variations in Ω (see also Rosenblum & Turvey, 1988).

In our previous research on absolute coordination, the focus has been on (a) the determinants of the frequency that the two units comfortably lock into for a given Ω (Kugler & Turvey, 1987; Turvey et al., 1988), (b) the dependence of mean phase on Ω (Rosenblum & Turvey, 1988), (c) the temporal and spatial fluctuations in the motions of an individual unit as a function of deviation from its characteristic frequency (Rosenblum & Turvey, 1988), (d) the independence of the timing of the interlimb coordination from the phasing of muscular activities driving the individual limbs (Turvey, Rosenblum, Schmidt, & Kugler, 1986; Turvey, Schmidt, & Rosenblum, 1989), and (e) the dependence of the coupled frequency and mean phase on nonspecific body stiffness (Bingham, Schmidt, Turvey, & Rosenblum, 1991). In the present article, the focus is on the dynamical substructure of 1:1 frequency locking. The guiding assumption is that the coordination can be viewed as a dynamical activity that is a consequence of many unseen layers of activity that are often related from one layer to the next by means of a scaling factor (Shlesinger, 1987; West & Shlesinger, 1989, 1990).

The dynamical activity is measured by the power spectra of relative phase. The relative position of an oscillator within a cycle is known as its phase angle ($\phi$). The phase angle is 0° at the beginning of the cycle and 360° at the end of the cycle. The relative phase of a pair of frequency-locked oscillators is the difference between the phase angles of the two individual

This research was supported by National Science Foundation Grant BNS-8811510 to M. T. Turvey.

We thank Eliot Saltzman, Brian Shaw, and an anonymous reviewer for their comments on an earlier version of this article.

Correspondence concerning this article should be addressed to R. C. Schmidt, Department of Psychology, 2007 Percival Stern Hall, Tulane University, New Orleans, Louisiana 70118.

oscillators ($\phi_1 - \phi_2$). Haken and colleagues (Haken, Kelso, & Bunz, 1985; Haken & Wunderlin, 1990) argued that relative phase is an ideal measure of the spatial–temporal order in interlimb coordinations. First, it defines an order parameter that accurately reflects the cooperativity between the individual limb motions and remains relatively invariant across variations in the individual limb motions (e.g., in velocity). Furthermore, relative phase captures qualitative changes in the spatial–temporal organization of interlimb coordination. In particular, experiments have shown that increasing the frequency of oscillation of the limbs when the phasing of limbs begins in the alternate phase mode produces a transition to the symmetric phase mode; no similar transition is produced, however, by increasing the frequency of oscillation when the phasing of limbs begins in the symmetric phase mode (Kelso, 1984). Haken et al. (1985) modeled relative phase as having a dynamic with point attractors at 0° and 180° that underlie the symmetric and alternate relative phase modes, respectively. They interpreted the transition phenomena in terms of a layout of point attractors that identify the two phase modes: The increase in frequency when the limbs are in the initial 180° phase mode produces an annihilation of the point attractor at 180° and causes a bifurcation to the 0° phase mode (see also Schmidt, Carello, & Turvey, 1990). A preliminary analysis of the consequences in the relative phase power spectrum of increasing the frequency of oscillation suggests peaks in the power spectrum at the frequency of oscillation, spectral broadening at the transition, and a foreshadowing of the new phase mode immediately before the transition (Kelso & Scholz, 1985). In what follows, we detail what can be expected of the relative phase power spectrum as a function of a different variable, namely, Ω—the ratio of (uncoupled) frequencies of the biokinematic links when the frequency of oscillation is kept at a constant, comfortable frequency.

## Circle Map Dynamics

There is a conceptual simplification of the coupling of two oscillators that provides insight into the achieving of mode locking with competing frequencies and that has implications for what may be expected in the spectrum of relative phase.[1] Let Φ and Ψ represent the phase angles of the two oscillators, with periods of P(Φ) and P(Ψ), and let the Ψ oscillator influence the Φ oscillator. The influencing is done through a periodic forcing of strength or amplitude $K$. When decoupled, the motions of the two oscillators can be represented on a torus with the phase of the Φ oscillator expressed as a function of the phase of the Ψ oscillator (Abraham & Shaw, 1982). A cross-section that intersects the smaller diameter of this torus gives a Poincaré map for the Φ oscillator:

$$\Phi_{n+1} = \Phi_n + 2\pi P(\Psi)/P(\Phi).$$

When the two oscillators are coupled through the periodic forcing with amplitude $K$, the Poincaré map becomes

$$\Phi_{n+1} = \Phi_n + 2\pi P(\Psi)/P(\Phi) - K \sin(\Phi_n),$$

where the function $K(\Phi)$ satisfies $K(\Phi + 2\pi) = K(\Phi)$ for all Φ. Substituting $2\pi\theta_n$ for $\Phi_n$ and Ω for P(Ψ)/P(Φ) yields

$$\theta_{n+1} = \theta_n + \Omega - (K/2\pi)\sin(2\pi\theta_n),$$

which is the mapping of the circumference of a circle (i.e., the cross-section of the torus represented as $\theta$, where $0 \leq \theta < 1$) to itself—a circle map. This circle map can be used to investigate mode-locking patterns in a prototypical system with two competing frequencies (Arnold, 1965, 1983; Jackson, 1989; Thompson & Stewart, 1986). Importantly, it has also been shown to describe oscillations with mutual rather than one-way forcing such as the periodic flows in hydrodynamic experiments (Fein, Heutmaker, & Gollub, 1985; Haucke & Ecke, 1987; Stavans, 1987).

For very small $K$, the asymptotic behavior of the iterated circle map tends to a unique attracting periodic fixed point whenever Ω approximates $p/q$ where $p$ and $q$ are integers (e.g., $p/q$ approximates closely 1/1, 1/3, etc.). Because $p$ and $q$ are defined above as the period of the forced and period of the forcing oscillators, this means that for $q$ cycles of the forcing oscillator, the forced oscillator will make $p$ cycles. At some Ω values farther from $p/q$, however, the periodic behavior may disappear. The forced oscillator may then exhibit phase drift or quasiperiodicity. This usually occurs when the coupling between the two oscillators is low (i.e., for small $K$ values). Figure 1 depicts both periodic and quasiperiodic behavior of the circle map. In the circle map, mode locking manifests itself through periodicity of the forced oscillator. That is, after $q$ iterations of the map, the new phase angle differs from the initial value by an integer $p$. Quasiperiodicity is due to the fact that Ω was outside of, or on the borders of, the window of Ω values defining the region of periodicity for the given value of $K$. Figure 2 (top panel) shows a number of periodic windows in the ($K$, Ω) plane. The bounded regions of mode locking are called *Arnold tongues* and represent synchronization resonances between the two frequencies. As can be seen, these regions increase in size with increasing $K$. This means that at higher $K$ values, mode locking becomes more probable. The probability increases until it is above some critical value, when the probability of mode locking becomes 1. This occurs in the region in which the resonances of the different Arnold tongues may overlap. The overlapping resonances can lead to chaotic behavior manifested as hysteresis effects (Jensen, Bak & Bohr, 1984) because different initial phase angles can lead to very different mode locks. Furthermore, from inspection of Figure 2 (top panel), if $K$ and Ω are controllable simultaneously, then for values of $K$ below criticality, it is possible to take a path in the ($K$, Ω) plane without entering any of the tongues and, therefore, without encountering mode locking.

The number labeling a given Arnold tongue in Figures 1 and 2 is called a *winding number*, defined as $W(K, \Omega) = (\theta_n - \theta_0/n)$ in the limit as the iteration $n$ approaches infinity (Jackson, 1989). The quantity $W$ represents the average increase in the angle $\theta$ per unit time (average frequency), and for a mode-locked situation, $W = p/q$. Thus a mode locked state exists when $W$ equals a rational number; when W is irrational, the state is quasiperiodic.

In the present article, we are interested in interlimb coordinations that are the equivalent of $W = 1{:}1$. Let us see the conditions under which a winding number of unity is achieved

[1] The following derivation of the circle map is taken from Jackson (1989).

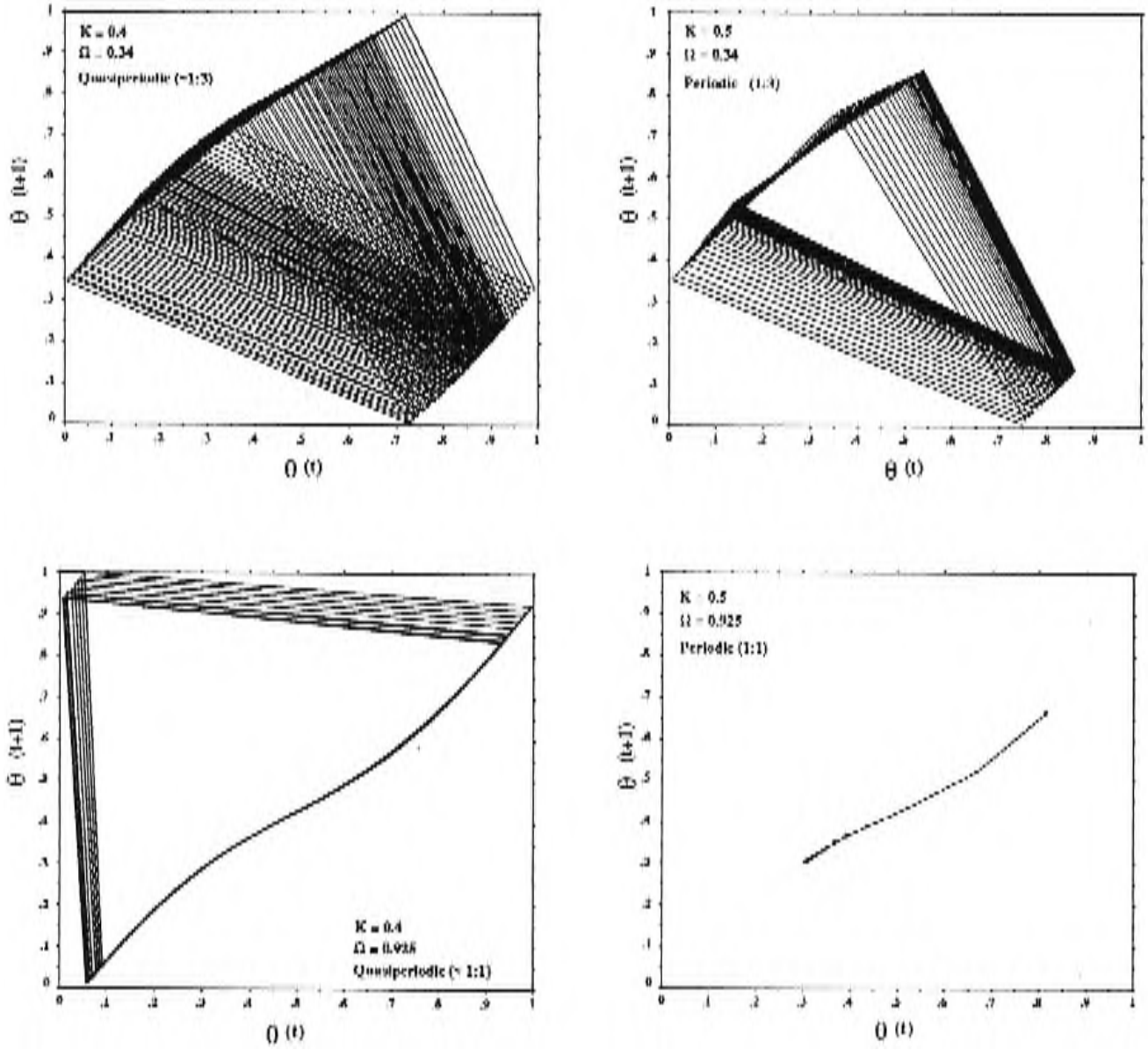


*Figure 1.* Return maps for 200 iterations of the circle map showing phase angle $\theta$ at time $t$, against $\theta$ at time $t + 1$. (For fixed $W = p/q$, $K$ can be varied to yield either quasiperiodic or exactly periodic motion. Successive phase angles are connected to depict evolution of phase. The left top panel shows that with $K = 0.4$ and $\Omega = 0.34$, quasiperiodic drift close to 1:3 phase lock occurs where the phase angle returns to a nearby phase angle, $\theta$, after three iterations [$W \approx 1{:}3$]. The top right panel shows that with $K = 0.5$ and $\Omega = 0.34$, periodic motion occurs [$W = 1{:}3$]. Following several transient iterations, phase angle returns to exactly the same $\theta$ after three iterations. The bottom left panel shows that with $K = 0.4$ and $\Omega = 0.925$, quasiperiodic drift close to 1:1 lock occurs [$W \approx 1{:}1$]. The bottom right panel shows that with $K = 0.5$ and $\Omega = 0.925$, periodic motion occurs [$W = 1{:}1$]. Following several transient iterations phase angle returns to a value of $\theta = 0.3$ on each iteration.)

in the circle map. Figure 2 (bottom panel) shows that when $K < 1$, the range of $\Omega$ values over which $W = 1{:}1$ is relatively small. For $K > 1$ (the chaotic region), the range is extended to encompass all $\Omega$ values. What is noticeable about the achievement of $W = 1{:}1$ across the full ($K$, $\Omega$) plane is that as $\Omega$ departs farther and farther from 1, the requisite $K$s increase in magnitude and decrease in range. Outside of the delimited range, the behavior is quasiperiodic (when $K < 1$) or possibly chaotic (when $K > 1$). In sum, where this particular circle map dynamic applies ($W = 1{:}1$), there is always a coupling value to be found such that oscillators of competing frequencies can oscillate together at the same compound frequency.

If absolute interlimb coordination were understandable as a circle map dynamic, then the challenge of this coordination would be that of discovering a specific coupling magnitude yielding 1:1 mode locking for a given value of $\Omega$. What are the constraints on satisfying this challenge? As noted, the band of K values yielding $W = 1{:}1$ mode locking compresses as $\Omega$ deviates more and more from 1 (see Figure 2, bottom panel). It is also the case that the $K$ values associated with

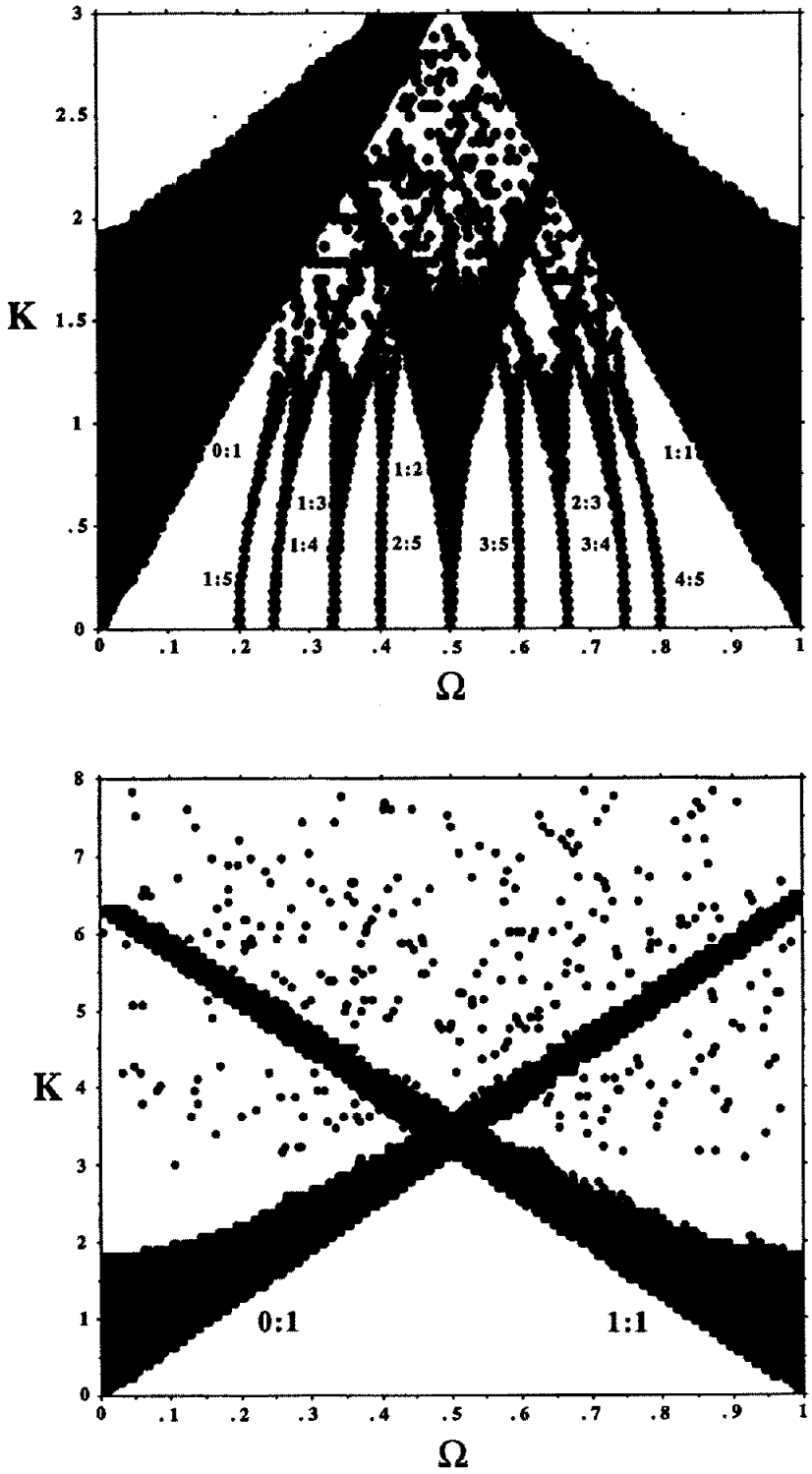


*Figure 2.* The top panel depicts phase space with Arnold tongues (in black), indicating phase locking regions with winding number, $W = p:q$, for frequency ratio $\Omega = 0$ to 1, and coupling $K = 0$ to 3; the bottom panel depicts phase-locked regions (broad black lines) for winding number $W = 0{:}1$ and $W = 1{:}1$. (Note how the Arnold tongue for $W = 1{:}1$ cuts across the complete range of possible frequency ratios as coupling, $K$, is increased. Note also how the width of the tongue narrows with deviation from $\Omega = 1$. The apparently randomly scattered regions show that periodicity also exists outside of the orderly regions.)

highly stable mode locking decrease in number as the band gets thinner (Schuster, 1988). The implication is that if absolute interlimb coordination were understandable as a circle map dynamic, then mode locking achieved at larger frequency differences would be likely to exhibit more fluctuations—as the probability of settling on unstable $K$ magnitudes increases. Given that the range of highly stable $K$ values decreases in approximately linear fashion, the implication, more fully, is that the fluctuations in mode locking as measured by variance in the relative phase should increase with deviations of $\Omega$ from 1. If this is true, then the question arises of the consequences of this increase in variance for the organization of subtasks underlying the mode locking. We turn our attention presently to techniques for investigating this organization of subtasks.

## Fractal Time

At its coarsest level, the wedding of two limbs in absolute coordination is describable as a single task of moving each limb at the same frequency. At a less coarse level, absolute coordination involves several subtasks, for example, sequential contractions of the flexors and extensors of one limb and sequential contractions of the flexors and extensors of the other limb. Insofar as these latter subtasks are nested within the task of 1:1 frequency locking of limb movements, they can be expected to occur at higher frequencies. As the grain size of analysis decreases further we can, of course, expect to identify more and more subtasks—those having to do with neuromotor and vascular processes, for example—and we can expect many of these finer subtasks to operate at shorter time scales. We can also expect subtasks whose time scales are longer than those of the interlimb coordination. An interlimb coordination of, say, 1 Hz performed for about 100 s will likely involve the following basic cyclic subtasks: (a) primary neural frequencies in the 50–5 Hz range, (b) a muscle motor unit frequency at about 10 Hz, (c) a heartbeat at about 1 Hz, (d) a ventilation rate at about 0.25 Hz, and (e) a capillary red blood cell flow acting as an oxygen choke limiting the rate of local oxidation in muscle tissue at about 0.01 Hz (Iberall, 1969).

The idea of potentially many subtasks having to be realized for the achievement of interlimb coordination is consistent with the homeokinetic thesis proposed by Iberall and colleagues that regulation of any macroscopic biological function is a cooperativity of many temporally quantized cyclic processes (Bloch et al., 1971; Iberall, 1977, 1978; Iberall, Soodak, & Hassler, 1978). The homeokinetic theory implies a spectroscopic approach to coordinated movement patterns. In general, a spectroscopic analysis reveals the relationship between the important repetitive processes going on within a system and the time domain in which they occur. Its exposition is in a conventional spectral plot that presents power or amplitude on the ordinate against frequency on the abscissa. For complex systems, such a representation shows how the energy of a process is distributed across different kinds of activities at different time scales.

Both local and global properties of the distribution of spectral energy can be found through spectroscopic analysis. First, spectral plots will often indicate different activities by a concentration of energy at specific frequencies, that is, by peaks in the power spectrum. Such local spectral landmarks may index task-specific, cyclic processes that are operating to help bring about a coordinated activity. Alternatively, spectral plots can demonstrate the global form of the distribution of energy across dynamical subtasks. What has been observed for complex systems consisting of multiple space–time scales is that the subtasks will be interrelated such that the amount of power at a given frequency is a function of the inverse of the frequency; that is, an ensemble's spectrum can be characterized by a relationship that scales the magnitude of activity to $1/f^{\delta}$, where $f$ is frequency and $\delta$ is a scaling factor. These spectra are called inverse power-law spectra. Spectra with inverse power-law distributions have been reported for a number of biological processes (e.g., Goldberger, Bhargava, West, & Mandell, 1985; Goldberger, Kobalter, & Bhargava, 1986; Koboyashi & Musha, 1982), including finger tapping (Musha, Katsurai, & Teramachi, 1985) and, perhaps, postural control (Aggashyan, Gurfinkel, & Fomin, 1973; Powell & Dzendolet, 1984), and are said to signify the balance between order and variability in biological processes (West, 1988; West & Goldberger, 1987; West & Shlesinger, 1989).

The inverse power-law spectrum is a manifestation of the fractal or scale-invariant nature of the underlying process (e.g., Feder, 1988; West & Shlesinger, 1990). Magnitudes of the scaling factor $\delta$ other than 1 have been noted in complex systems (West & Shlesinger, 1990). What the magnitude of this scaling factor indicates is the degree that the power is concentrated at the lower frequencies of the spectrum. A spectrum that scales power to $1/f^0$ is a flat spectrum of white noise. Such a spectrum has the same amount of power everywhere and represents a random organization of subtasks: Fluctuations at any moment are independent of fluctuations at any other moment. As $\delta$ grows in magnitude, the distribution of the power becomes nonuniform, with more of the total power being relegated to the lower frequencies. The $1/f$ spectrum ($\delta = 1$) represents a state of organization such that each frequency has power proportional to the inverse of its frequency (or equivalently, power proportional to its period of oscillation). Hence, processes with longer time scales have more spectral power associated with them. Furthermore, because this power is not concentrated at a certain portion of the spectrum but is distributed across the entire spectrum, fluctuations at one time scale are only loosely correlated with those of another time scale.[2] Hence, this linear distribution of energy with the inverse of frequency makes the system "more adaptive to internal changes and to changes in the environment" (West & Shlesinger, 1990, p. 44) such that a perturbation to a process at one time scale will not necessarily influence the global integrity of the entire system.

For the general case of biological systems, it has been argued that subtasks will be weakly correlated and the distribution of power in the spectrum should scale to $1/f^1$ (Iberall et al., 1978). The $1/f$ spectrum lies midway between the flat spectrum of white noise ($1/f^0$) and the steep spectrum of Brownian

[2] If the power of a spectrum is represented only at a single frequency, the behavioral fluctuations of the system will be perfectly correlated.

noise ($1/f^2$). Because the bulk of the total power is concentrated below 1 Hz, Brownian noise has fluctuations that are strongly correlated over this characteristic time scale. As such, these organizations are less adaptive to perturbation induced internally and externally.

Presumably, the picture of multiple subtasks at multiple time scales holds for any kind of biological coordination, including interlimb absolute coordination. Furthermore, this picture should hold for the frequency locking of biological oscillators regardless of parameterizations such as $\Omega$. The question to be addressed in this article, using spectroscopy, is how the dynamical substructure underlying this frequency locking meets the challenge of differences in $\Omega$. How does $\Omega$ affect the organization of necessary subtasks used to bring about the frequency-locked state?

Given the circle map analysis of frequency-locking phenomena above, we may expect that a deviation of $\Omega$ from 1 reduces the stability of the frequency-locked regime. Hence, what might differ with $\Omega$ is the amount of overall activity in the relative phase spectrum, namely, the total power. This increase in total power may also be accompanied by changes in the way the power becomes distributed (both locally and globally) within the relative phase spectrum. For example, the increase in the energy of the power spectrum may be concentrated locally at specific frequencies of task-specific processes that are required to maintain stability of the system as a whole. In this case, new spectral peaks should appear that represent these task-specific processes, and their magnitude should increase with deviation of $\Omega$ from 1. Furthermore, assuming that the distribution of spectral energy will follow an inverse power law, we could expect that the scaling factor $\delta$ will change to reflect a change in stability caused by the deviation of $\Omega$ from 1. For example, we might expect to see $\delta$ decrease in magnitude. This indicates that the fluctuations at the different time scales are becoming increasingly less correlated. A reasonable claim is that the subtasks are most tightly related when $\Omega = 1$; they are bound together by nonlinear interactions such that fluctuations in any one subtask are met by compensatory fluctuations in others. Consequently, the spectra of interlimb coordinations at $\Omega = 1$ and values close to it should be characterized by fluctuations that are strongly correlated, meaning that we might expect spectral power to scale as $1/f^{\delta}$, where $\delta$ is 2 or more. If increasing frequency competition reduces the degree of correlation among the fluctuations at the various time scales, then there should be a systematic decrease in the slope of the Log Power × Log Frequency function with increased deviations from $\Omega = 1$.

In sum, the above considerations of circle map dynamics and fractal time suggest the following predictions. For interlimb coordination, where the two limbs (wrist–pendulum systems) satisfy $W = 1{:}1$, an index of the state of coordination such as the power spectrum of relative phase may (a) exhibit an inverse power law given by the term $1/f^{\delta}$, where $\delta$ is a positive number; (b) increase in variability (total power) with increasing deviation of $\Omega$ from 1; (c) exhibit more spectral peaks with increasing deviation of $\Omega$ from 1; and (d) exhibit reduction in the scaling exponent $\delta$ with increasing deviation of $\Omega$ from 1.

## Method

The foregoing predictions are evaluated with the data from a study consisting of six separate sessions (or experiments) conducted over a 21-month interval with the same 3 subjects. The study was designed to address simultaneously a number of different issues concerning absolute coordination. Some methodological details and results of the study have already been reported (Kugler, Turvey, Schmidt, & Rosenblum, 1990; Rosenblum & Turvey, 1988; Turvey et al., 1989; Turvey et al., 1988). The emphasis in what follows is on the features of the experimental design that bear directly on questions concerning the fluctuations in relative phase as a function of $\Omega$.

### *Subjects*

Three male subjects participated in all six sessions. Two were graduate students at the University of Connecticut and one was a faculty member.

### *Materials*

The pendulum construction and the optical recording procedure were as described in Kugler and Turvey (1987), Turvey et al. (1986), and Rosenblum and Turvey (1988).

Table 1
*Frequency of the Constant Right Wrist–Pendulum System, Frequency Range of the Variable Left Wrist–Pendulum System, and Range of $\Omega$ Values as a Function of Subject and Session*

| | Subject 1 | | | Subject 2 | | | Subject 3 | | |
|---|---|---|---|---|---|---|---|---|---|
| | Pendulum frequencies | | $\Omega$ | Pendulum frequencies | | $\Omega$ | Pendulum frequencies | | $\Omega$ |
| Session | Right | Left range | range | Right | Left range | range | Right | Left range | range |
| 1 | 0.89 | 1.17–0.74 | 0.84–1.30 | 0.89 | 1.17–0.74 | 0.84–1.31 | 0.90 | 1.19–0.75 | 0.84–1.31 |
| 2 | 0.89 | 1.45–0.62 | 0.71–1.64 | 0.89 | 1.47–0.62 | 0.70–1.66 | 0.90 | 1.52–0.63 | 0.70–1.69 |
| 3 | 1.08 | 1.45–0.62 | 0.57–1.34 | 1.09 | 1.47–0.62 | 0.58–1.36 | 1.11 | 1.52–0.63 | 0.57–1.38 |
| 4 | 0.76 | 1.45–0.64 | 0.84–1.91 | 0.76 | 1.47–0.64 | 0.84–1.93 | 0.77 | 1.52–0.64 | 0.83–1.98 |
| 5 | 1.29 | 0.97–0.57 | 0.45–0.76 | 1.29 | 0.98–0.57 | 0.44–0.76 | 1.32 | 0.99–0.57 | 0.43–0.75 |
| 6 | 1.43 | 0.97–0.57 | 0.39–0.68 | 1.45 | 0.98–0.57 | 0.39–0.67 | 1.50 | 0.99–0.57 | 0.38–0.66 |

*Note.* $\Omega = \sqrt{\text{right length}_s/\text{left length}_s}$ = left frequency/right frequency because $f = \frac{1}{2}\pi(g/l)^{1/2}$. Frequency is in Hz and is computed for each system considered as a strictly gravitational pendulum.

In each session of the study, the right wrist pendulum was of fixed magnitude, although this magnitude varied across sessions. Different Ω were produced by varying the magnitude of the left wrist pendulum. The characteristic frequencies of both the (constant) right systems considered as strictly gravitational pendulums and the range of characteristic frequencies for the (variable) left systems considered as strictly gravitational pendulums are reported in Table 1 together with the corresponding range of Ω values (left/right) for each subject in each of the six sessions of the study. Because the masses of the subjects' hands enters into the computations of these simple gravitational pendulum equivalents of wrist–pendulum systems (Kugler & Turvey, 1987), the characteristic frequencies differ for the 3 subjects.

### *Procedure*

Subjects (run 1 at a time) sat on a stool with their feet planted firmly on a foot stand. They were given extensive verbal instructions in the first session. Each subject was instructed to hold his forearms parallel to the ground plane and to gaze straight ahead without looking at either wrist–pendulum system. Subjects were asked to oscillate the pendulums forward and backward smoothly, using only the wrist joints while gripping each pendulum's handle so as to have complete control over the entire swing. The subject was told to swing the pendulums in alternate fashion (i.e., at 180° relative phase angle, with one pendulum moving forward and simultaneously the other pendulum moving backward) with a single, most comfortable common period. Importantly, before the recording of each trial, the subject was given as long as needed to settle on a tempo that he felt was comfortable and stable. Each recorded trial lasted for 15 s, except in Session 6, in which the trials were of 10 s duration. The set of instructions was repeated to subjects in briefer form for Experimental Sessions 2–6; subject behavior was monitored closely throughout the six sessions.

In Sessions 2–5, there were eight absolute coordination conditions and one single right wrist–pendulum condition. In Sessions 1 and 6, there were 11 absolute coordination conditions and one single right wrist–pendulum condition. To reiterate, the right system was held constant across the absolute coordination conditions of each session. (The single right wrist–pendulum condition in each session permitted the determination of the right system's preferred period, a measure that was needed for other experimental questions but not those raised here.) In Sessions 1, 2, and 5, there were eight trials per condition; in Sessions 3 and 4, there were four trials per condition, and in Session 6, there were six trials per condition. For each session, the total trials were divided into a number of blocks, each of which involved one trial of every condition type. Trials within each block were given a random ordering, and this ordering was different for each subject. The sessions varied in length from about 1.5 to 3.4 hr (depending on the number of trials involved), including a 15-min break that occurred halfway through each session. The six sessions spanned 21 months with an average interval of 3 months between sessions.

### *Analyses*

The effective mass and length of a single wrist–pendulum system were calculated as the equivalent simple pendulum mass and length of the compound pendulum consisting of the attached mass, the dowel, and the hand of the subject, using the methods described in Kugler and Turvey (1987) and Turvey et al. (1986).

The digitized displacement time series of the wrist–pendulum systems were smoothed by using a Bartlett (triangular) moving average procedure with a window size of 35 ms. Each trial was subjected to software analyses to determine the coordination frequency of oscillation of each wrist–pendulum system (right and left), the time series of the relative phase between the two wrist–pendulum systems, the power spectra of this relative phase time series, the total power associated with each of these spectra, and the mean of the relative phase time series.

A peak-picking algorithm was used to determine the time of peak flexion and extension of the wrist–pendulum trajectories. From the peak extension times, the frequency of oscillation for the $n$th cycle was calculated as

$$f_n = 1/(\text{time of peak extension}_{n+1} - \text{time of peak extension}_n).$$

The mean of these cycle frequencies was calculated to produce the mean frequency of oscillation for each wrist–pendulum system for each trial. The mean frequency of oscillation for each condition (each pairing of wrist–pendulum systems) was then calculated from the trial means.

The difference between the phase angles of each wrist–pendulum system was calculated for each sample (200/s) of the displacement time series to produce a time series of the relative phase angle. The phase angles at sample $i$ ($\phi_i$) were calculated as

$$\phi_i = \arctan(\dot{x}_i^*/\Delta x_i),$$

where $\dot{x}_i^*$ is the velocity of the time series at sample $i$ divided by the mean angular frequency for the trial, and $\Delta x_i$ is the displacement of the time series at sample $i$ minus the average displacement for the trial. The relative phase angle that the subject intended to produce was 180°. The relative phase time series allows an evaluation of how the subject satisfied this task demand. The evaluation was accomplished in a number of ways. First, the mean of the relative phase was calculated for each trial and condition. Second, to determine the magnitude and patterning of the variability associated with this time series, a power spectral analysis was performed on the relative phase time series. The data first were windowed by using a Welch filter to reduce spectral leakage, and all of the trial spectra from a given condition were averaged to reduce the error of the spectral estimate (Press, Flannery, Teukolsky, & Vetterling, 1988). Third, the total power of relative phase was calculated for each condition by summing the power at each frequency of the averaged spectra except the DC component at the zero frequency. This measure was used as a summary of the variability of the relative phasing of the left and right wrist–pendulum systems.

## Results and Discussion

### *1:1 Frequency Lock*

Figure 3 plots $W$ against Ω for each of the 3 subjects. For each condition, $W$ was calculated as the ratio of the frequency of the right unit and the frequency of the left unit. Ω was calculated as

$$\Omega = \sqrt{\text{right length}_s/\text{left length}_s},$$

where right length$_s$ is the equivalent simple pendulum length of the right unit and left length$_s$ is the equivalent simple pendulum length of the left unit. This quantity is equivalent to a measure of the ratio of uncoupled frequencies on the assumption that each wrist–pendulum system can be considered a purely gravitational pendulum ($f = \frac{1}{2}\pi(g/l)^{1/2}$). As is evident from inspection of Figure 3, $W$ always approximated unity and did so independently of Ω.

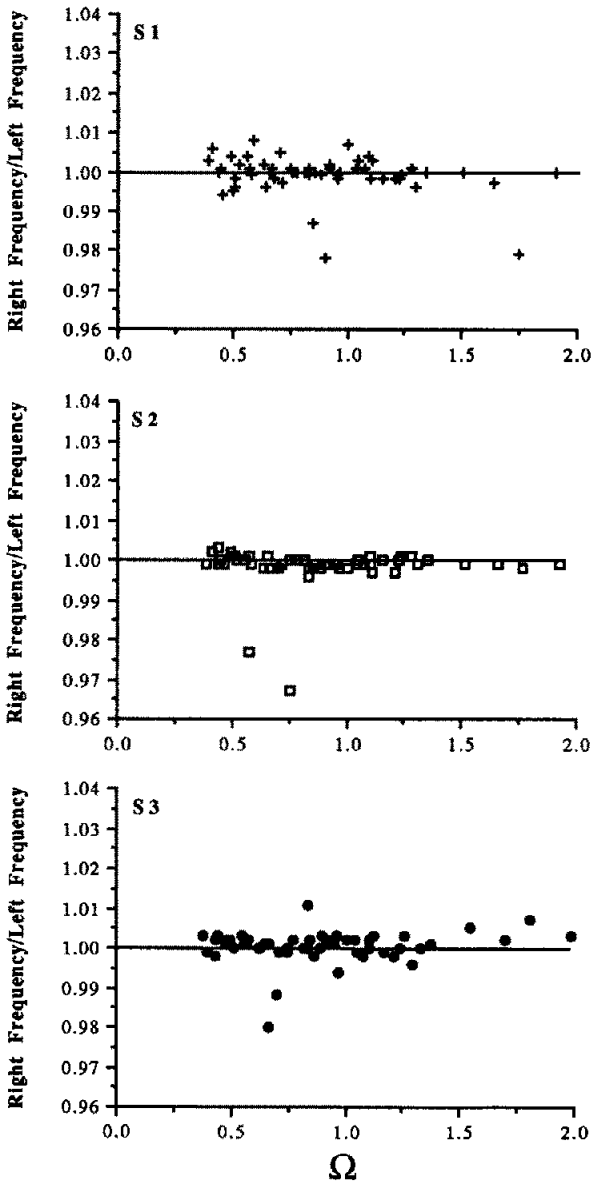


*Figure 3.* The ratio of right and left wrist–pendulum frequencies of oscillation during 1:1 frequency locking as a function of Ω, the ratio of uncoupled frequencies of component wrist–pendulum systems.

## *Relative Phase*

Again, the subject's task was to oscillate the two wrist–pendulum systems in antiphase (at 180°). Figure 4 (top panel) shows the frequency distribution of mean phase angle. The subjects approximated their task with some amount of error. Figure 4 (bottom panel) shows that the mean phase usually departed from 180° as a function of Ω. The overall mean state of the relative phase was affected by the uncoupled frequency difference of the two wrist–pendulum systems: Larger differences in the frequencies (deviations of Ω from 1) produced greater deviations in relative phase from 180°. This observation on the present data set was reported previously by Rosenblum and Turvey (1988). In the present article, we add that the examination of the relative phase at the time scale of sampling (200 Hz) rather than at the time scale of a trial (15 s) reveals that phase angle is not static but changes in a complex manner within and across cycles. Figure 5 gives three examples of the relative phase time series for each subject at different values of Ω.

## *Local Patterning of the Relative Phase Spectrum*

*Power spectra of relative phase.* Figure 5 suggests that the mean relative phase angle is not sufficient in summarizing the full behavior of the relative phasing of frequency-locked biological oscillators. In satisfying the task criteria of comfortable 1:1 frequency locking and antiphase interlimb coordination, the moment-to-moment phasing of right and left pendular motions involved one or more cyclic components. This suggestion was evaluated through power spectral analy-

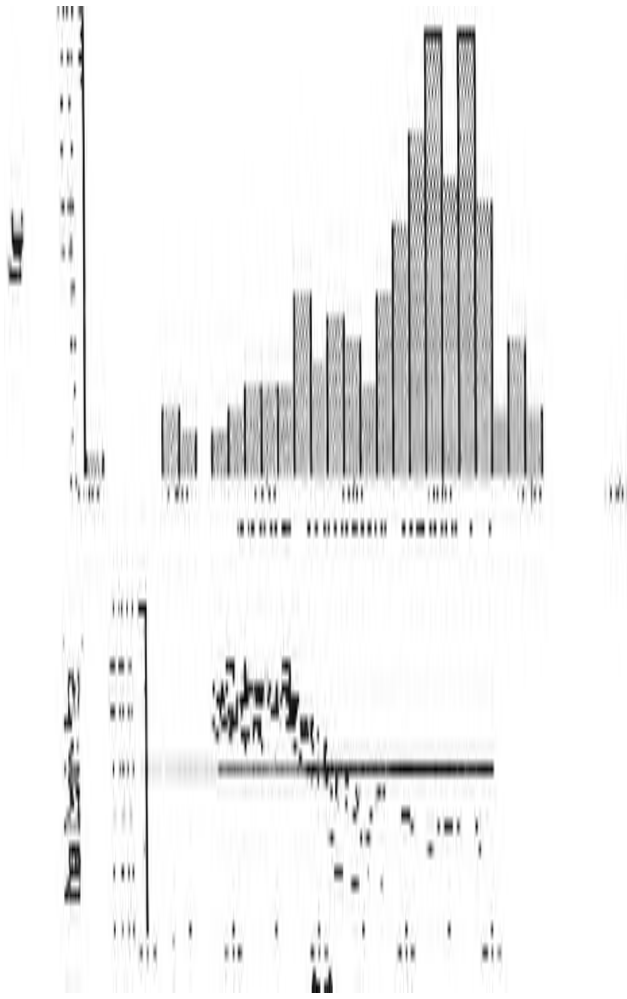

*Figure 4.* Frequency distribution of mean relative phase angles observed (top) and the mean relative phase angle plotted against Ω (bottom) for the data of the 3 subjects combined over the six sessions.

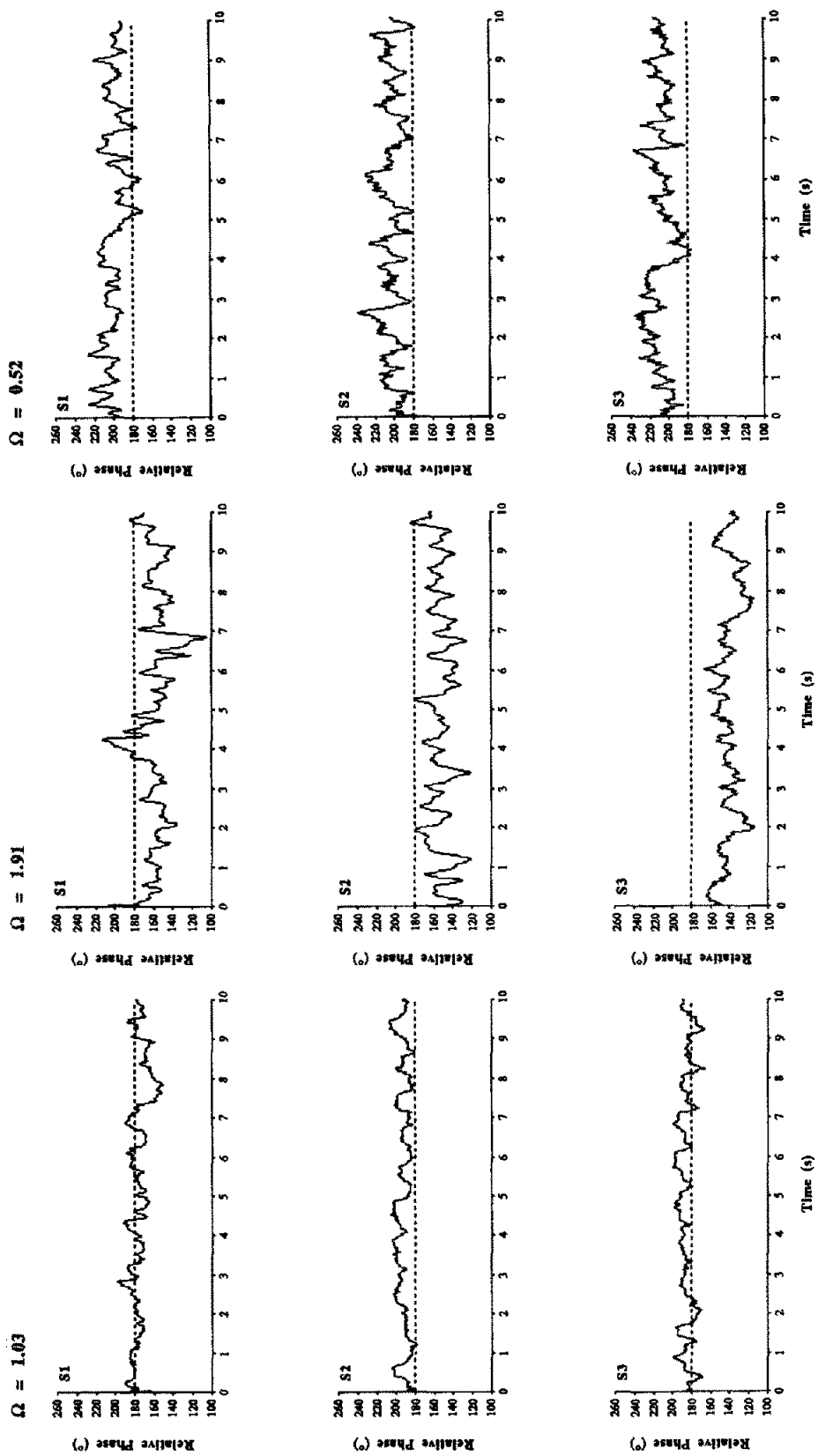


*Figure 5.* Typical time series of the relative phase for three different values of Ω. (Left panels: Ω = 1.03 defines a condition in which the uncoupled frequencies are almost identical. Oscillation periods for Subjects 1–3 are 1.100 s, 0.923 s, and 0.983 s, respectively. Middle panels: Ω = 1.91 defines a condition in which the left unit has a higher uncoupled frequency than the right unit. Oscillation periods for Subjects 1–3 are 1.076 s, 1.121 s, and 1.158 s, respectively. Right panels: Ω = 0.52 defines a condition in which the right unit has the higher uncoupled frequency. Oscillation periods for Subjects 1–3 are 1.291 s, 1.166 s, and 1.182 s, respectively.)

sis. Within a session, the power spectra for all of the trials of a given Ω were averaged as described above. Within these spectral plots, power was expressed as a function of normalized frequency, that is, frequency in units of the modal or coupled frequency, $f/f_{modal}$. These power spectra of the relative phase time series reveal predominant frequency components at integer multiples of the frequency of mode locking ($f_{modal}$) and at frequencies below the mode-locked frequency. They also seem to reveal that the prominence of the power of a given integer multiple depends on Ω. Figure 6 shows characteristic power spectra for three values of Ω for each of the 3 subjects.

To validate that the spectral peaks occur primarily at integer values of $f/f_{modal}$, an algorithm was constructed to determine the frequency at which the spectral peaks occurred, using for the criterion of a spectral peak an inflection point in the power with a magnitude greater than 1 deg$^2$. The candidate peaks were verified as peaks by using graphical representations of the spectra. Figure 7 provides a frequency count of the spectral peaks for all of the trials for all 3 subjects. Inspection of this plot reveals that the peaks occurred predominantly at or near integer values.

The observed characteristics of the power spectra bring into question the generality of modeling the dynamics of interlimb phase relations by point attractors (Haken et al., 1985). From the present evidence, it appears that the antiphase relation between two limbs has periodic components and may obey a more complicated dynamics. For example, the dynamics underlying the relative phase may be a limit cycle or several limit cycle attractors. The observed power spectra also bring to the fore questions about the processes that produce the spectral peaks. Do they correspond to rhythmic subtasks? If so, where do these subtasks operate within a cycle of interlimb coordination? How are they related? Why do most of them occur at frequencies that are integer multiples of $f_{modal}$? How much do they dominate the total power of the spectrum? Does the magnitude of the power of these subtasks change with Ω? In the next section, we initiate an evaluation of the last two questions.

*Power as a function of* Ω. The total power of a spectrum represents the amount of variability that is in the spectrum. Given the considerations of the circle map dynamics above, one may expect the total power of the relative phase spectrum to be related to Ω. Figure 8 (top panel) presents total power as a function of Ω for the 3 subjects combined in the range $\Omega \leq 1$. This range encompassed 68% of the data points. Three data points per subject were eliminated from this analysis because their magnitudes were aberrantly high. Linear regression analysis revealed that for the 3 subjects there was a systematic increase in variability in the range $\Omega \leq 1$ as Ω decreased from 1, $r^2(99) = .33$, $p < .001$. The range of $\Omega \geq 1$ revealed no significant increase of total power with Ω.

Generally, the variability represented by the total power may be distributed coherently in the form of spectral peaks at specific frequencies or more generally as a broadband elevation at all frequencies. The question remains whether the increase in total power with a decrease of Ω from 1 was a consequence of a general elevation of the spectra or an increase of the power at the spectral peaks. To evaluate this, the total power was partitioned into the portion of the total power exhibited by the peaks and the portion of the total power that is nonpeak (including the power on the sides of the spectral peaks). These two quantities are plotted against Ω in Figure 8 (middle and bottom panels, respectively). The result of these analyses is clear. The portion of the total power exhibited by the peaks increased with decrease of Ω from 1, $r^2(99) = .28$, $p < .001$, whereas the portion of total power that is nonpeak did not increase, $r^2(99) = .02$, $p > .05$. Furthermore, neither the peak power nor the nonpeak power changed significantly with Ω for the range of $\Omega \geq 1$ ($p > .05$). Hence, the increasing difference in the uncoupled frequencies of the wrist pendulums (Ω) that are to be 1:1 frequency locked increases the power that is coherently distributed at specific frequencies rather than the power at all frequencies of the spectrum. Under the assumption that the portion of the total power exhibited by the peaks is representative of interlimb rhythmic subtasks, this result implies that increases in Ω caused increases in the activity of these subtasks as a group.

*New spectral peaks as a function of* Ω. The activity of these subtasks may increase with Ω as a group, but does this mean that the same spectral peaks grow in magnitude or that new spectral peaks are added? Does the inclusion of rhythmic subtasks at integer multiples of the $f/f_{modal}$ vary with Ω? To investigate this, the maximum power in a 0.25 range surrounding each integer multiple (0.5, 1, 2, 3, 4, 5) of $f/f_{modal}$ was found for each spectrum of each subject. (Given that there were 54 conditions, the total number of computed peak power values was 54 × 6.) Log of these power values was regressed simultaneously on $|\log \Omega|$ of the condition of the spectrum and $\log f/f_{modal}$ (the integer multiple) of the spectral peak. These multiple regressions yielded the following equations for the 3 subjects: Subject 1, $\log P = -2.26 \log f/f_{modal} + 1.41 |\log \Omega| + 1.11$, $r^2(321) = .87$; Subject 2, $\log P = -2.56 \log f/f_{modal} + 3.59 |\log \Omega| + 0.66$, $r^2(321) = .87$; Subject 3, $\log P = -2.56 \log f/f_{modal} + 2.07 |\log \Omega| + .92$, $r^2(321) = .88$. For all 3 subjects, the coefficients on both independent variables were significant at the .001 level.

The implication of these analyses is that the amount of power at the integer multiples of $f/f_{modal}$ is a function of Ω and the magnitude of the integer multiple: Power becomes concentrated at the higher multiples of $f/f_{modal}$ as Ω increases. The increase in Ω causes new peaks (subtasks?) to appear. To demonstrate the tendency for new peaks to arise at larger deviations of Ω from 1, a figure can be constructed for each subject in which power is plotted against Ω for each spectral peak, with the power value for a given Ω determined by the above regression equation. Such a figure presents a family of curves with the curve for the 0.5 peak being the highest in the $\log P$ by $|\log \Omega|$ plane and the curve for the 5 peak being the lowest. Inspection of such a figure suggests that given a criterial value for what will be accepted as a peak, the higher frequencies will generally exhibit peaks only at the larger deviations of Ω from 1. Figure 9 presents the family of curves just described for 1 of the subjects; it is typical of the family of curves for all subjects. The results presented in Figures 8 and 9 suggest that the adding of subrhythms with deviations

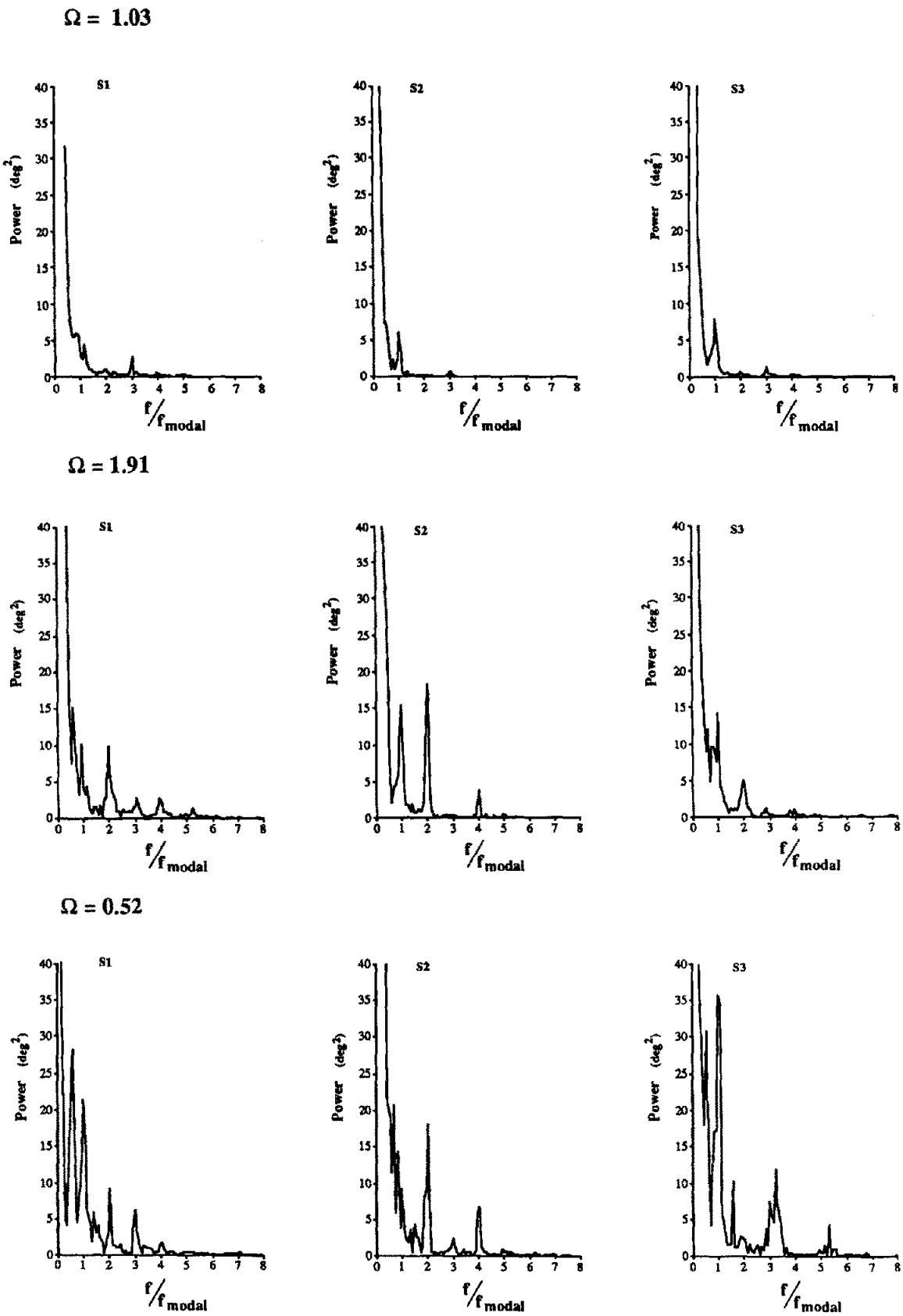


*Figure 6.* Typical normalized spectra of the relative phase for three different values of Ω. (Top panels, Ω = 1.03; middle panels, Ω = 1.91; bottom panels, Ω = 0.52.)

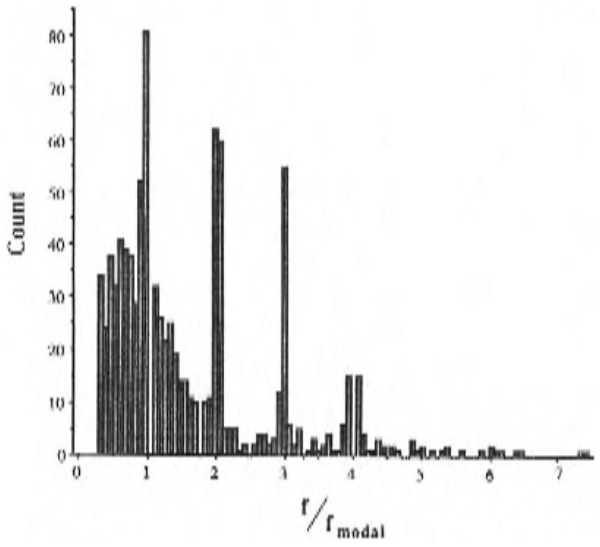


*Figure 7.* Frequency distribution of the peaks of the normalized spectra for the data of the 3 subjects combined over the six sessions.

of Ω from 1 is a systematic process. Because the same results were obtained for all 3 subjects, the implication is that the process in question is a preferred dynamical design property of human movement systems and, perhaps, of biological movement systems more generally.

Heretofore the analysis has focused on how the power in the relative phase spectrum was distributed locally and how these concentrations changed with Ω. What was found was that (a) the total power increased with decreases of Ω from 1, (b) the total power was concentrated mainly at integer multiples of $f_{modal}$, (c) the changes of power at these peaks were responsible for the changes of total power with decreases of Ω from 1, and (d) local concentrations of power at integer multiples were added at higher integer multiples as Ω decreased from 1. We now focus on the global patterning of the power across the entire spectrum by investigating the scaling of the power with frequency and how these scalings change as a function of Ω.

## *Global Patterning of the Relative Phase Spectrum*

*$1/f^{\delta}$ patterning of power.* Examples of power against normalized frequency ($f/f_{modal}$) in double logarithmic coordinates are shown in Figure 10, together with the linear regressions. Inspection reveals that the power spectra conform to a $1/f^{\delta}$ scaling. The exponent $\delta$ and coefficient $\alpha$ of the power formula relating spectral power to spectral frequency, $P = \alpha(1/f^{\delta})$, were determined for all 54 conditions for each subject. All 162 $r^2$ values were significant at $p < .001$; $\delta$ ranged from 1.64 to 2.96, with $M = 2.52$ and $SD = 0.26$; $\alpha$ ranged from 1.17 to 20.89, with $M = 4.57$ and $SD = 1.99$. Figure 11 presents the frequency distributions for $\delta$ and $\alpha$. The $\delta$ and $\alpha$ characteristics for the individual subjects are presented in Table 2. The size of $\delta$ suggests that fluctuations in relative phase were strongly correlated for all conditions. An important question is whether the strength of that correlation varied with Ω.

*Reduction in $\delta$ with increase in Ω.* Both $\delta$ and log $\alpha$ relate systematically to Ω. A second-order polynomial regression found the following relation in the overall data between $\delta$ and

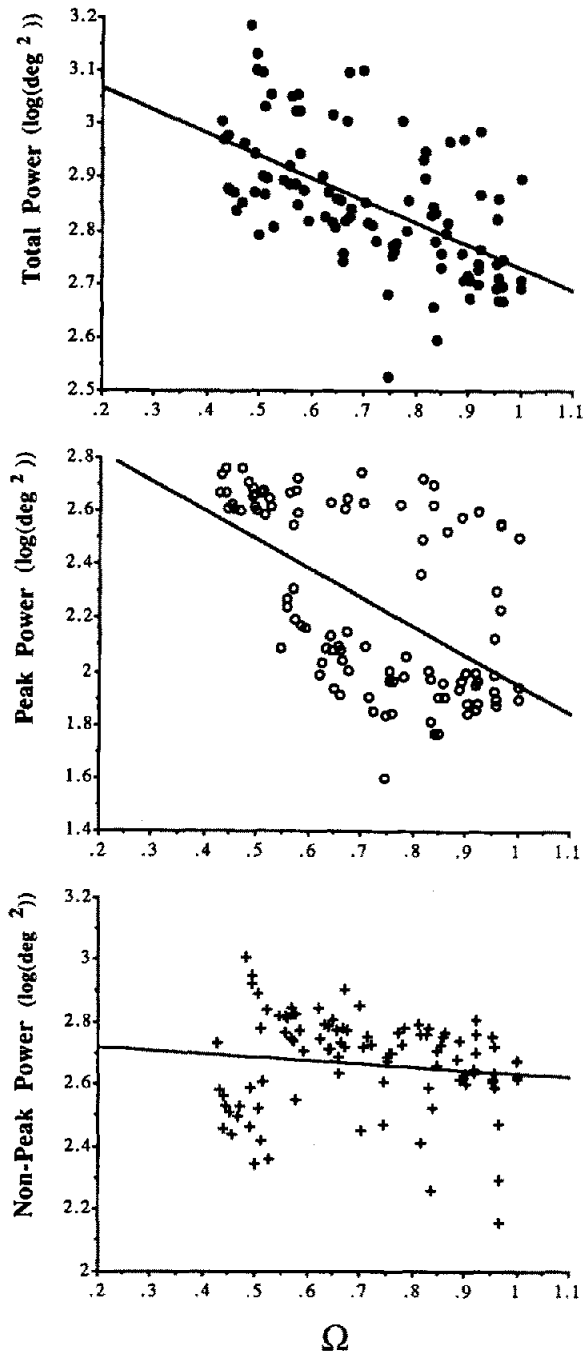


*Figure 8.* Total power, peak power, and nonpeak power of the relative phase spectra plotted as a function of Ω. (Significant increases as Ω deviated from 1 were found for total power [$y = -0.42\Omega + 3.15$, $r^2 = .33$] and for peak power [$y = -1.10\Omega + 3.05$, $r^2 = .32$] but not for nonpeak power.)

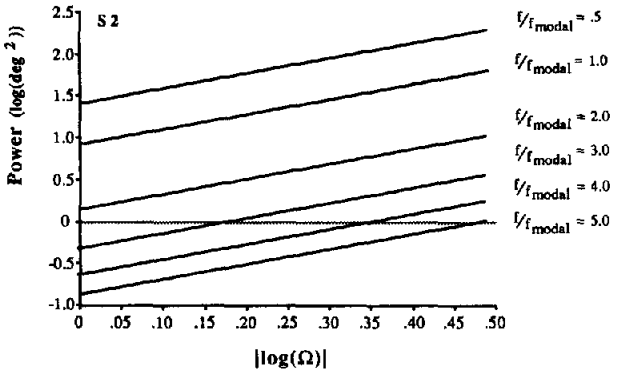


*Figure 9.* Power at integer multiples of the normalized relative phase spectra as a function of |log Ω| plotted for the $f/f_{modal}$ peaks at 0.5, 1.0, 2.0, 3.0, 4.0, and 5.0.

Ω: $\delta = -1.61 - 1.75\Omega + 0.71\Omega^2$, $r^2(161) = .36$, $p < .001$. Similar relations were found for the data of each subject taken individually. A second-order polynomial regression analysis found the following relation in the overall data between log $\alpha$ and Ω: $\log \alpha = 1.98 - 2.49\Omega + .97\Omega^2$, $r^2(161) = .63$, $p < .001$. Again, similar relations were found for the data of each subject taken individually. In sum, there seemed to be an approximately quadratic relation between $\delta$ and Ω and between log $\alpha$ and Ω, with a minimum in the vicinity of $\Omega = 1$.

To further the understanding of these dependencies, simple linear regression analyses were conducted for the range $\Omega \leq 1$. As mentioned above, most data fell within this range, as a matter of the design of the sessions; that is, for most conditions the left pendulum was larger than the right pendulum. For the overall data, $\delta$ decreased as Ω decreased from 1: $\delta = 1.88 + 0.86\Omega$, $r^2(109) = .32$, $p < .001$. For the individual subjects, the regressions were the following: Subject 1, $\delta = 2.04 + 0.49\Omega$, $r^2(35) = .19$, $p < .01$; Subject 2, $\delta = 1.36 + 1.56\Omega$, $r^2(35) = .66$, $p < .001$; Subject 3, $\delta = 2.02 + 0.57\Omega$, $r^2(35) = .27$, $p < .01$. Similarly, with respect to log $\alpha$ and Ω, log $\alpha$ increased as Ω decreased from 1. The linear regression on the overall data yielded $\log \alpha = 1.61 - 1.25\Omega$, $r^2(109) = .65$, $p < .001$. For the individual subjects, the regressions were the following: Subject 1, $\log \alpha = 1.53 - 0.97\Omega$, $r^2(35) = .64$, $p < .001$; Subject 2, $\log \alpha = 1.72 - 1.55\Omega$, $r^2(35) = .84$, $p < .001$; Subject 3, $\log \alpha = 1.59 - 1.26\Omega$, $r^2(35) = .73$, $p < .001$.

The observation that $\delta$ decreases with deviations of Ω from 1 is consonant with the hypothesis that the correlations between the subtasks sustaining 1:1 frequency locking weaken as the difference between the two uncoupled frequencies gets larger. Alternatively, it might be claimed that the attainment of 1:1 frequency locking with highly competitive frequencies is achieved through an organization in which the subtasks are more weakly correlated to accommodate increasing internal perturbations.

*Relation among individual spectra suggests a common, nonspecific subtask.* There was a negative relation between $\delta$ and log $\alpha$: In linear coordinates, $\delta = 2.89 - 0.56 \log \alpha$, $r^2(161) = .43$, $p < .001$. As the intercept of the Log $P \times$ Log $f/f_{modal}$ function got larger, the slope of the function got shallower. The implication is that slopes and intercepts were not affected independently by Ω and that there was a tendency for the inverse functions to form a convergent family. Theoretically, the 162 functions pass through a common point. It is possible to obtain an objective estimate of the point at which the functions intersect (Stevens, 1974; Stevens & Rubin, 1970). For any pair of intersecting functions, $P = \alpha_1(f/f_{modal})^{\delta 1}$ and $P = \alpha_2(f/f_{modal})^{\delta 2}$, it follows from the equal-

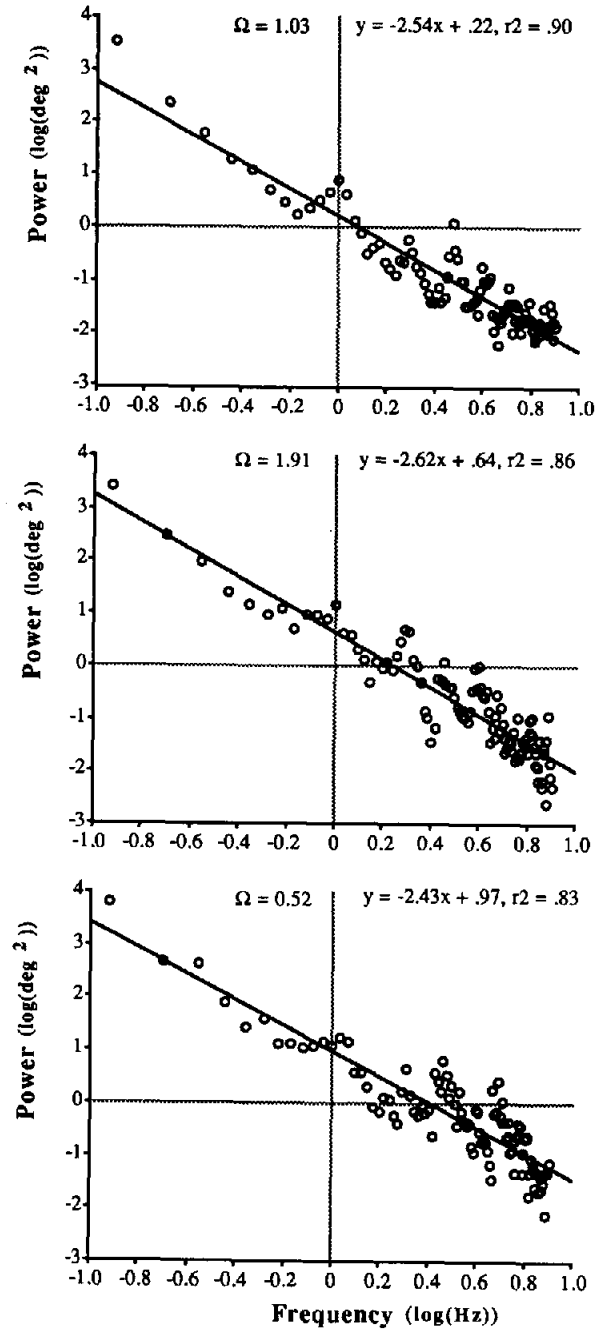


*Figure 10.* Log–log plots of the normalized relative phase spectra at three values of Ω for a typical subject.

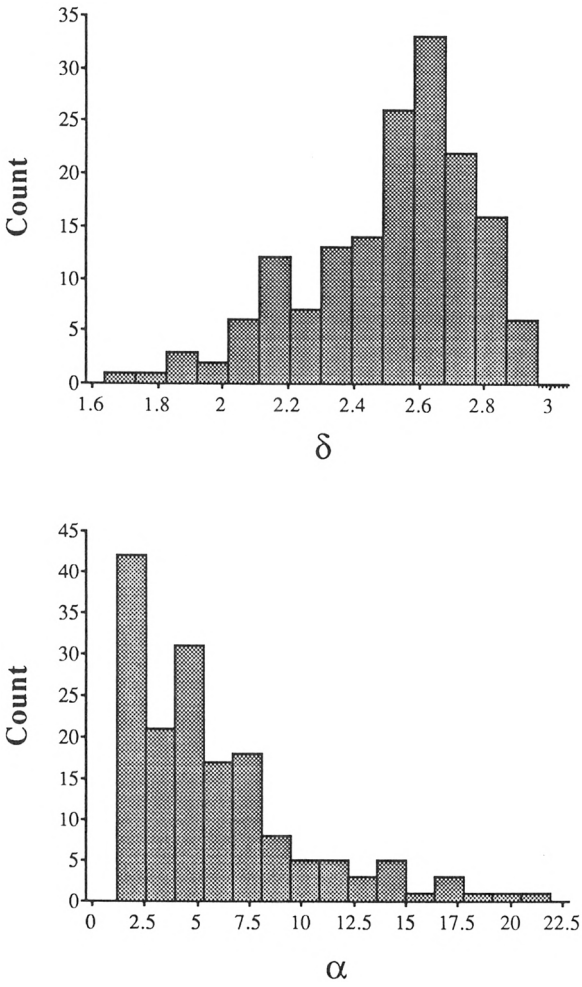


*Figure 11.* Frequency distributions $\delta$ and $\alpha$ for the data of the 3 subjects combined over the six sessions.

ity of power at the intersection point that

$$\alpha_1 f/(f_{\text{modal}}{}^{\delta 1}) = P = \alpha_2 f/(f_{\text{modal}}{}^{\delta 2}).$$

On taking the logarithm of this equation and rearranging terms,

$$(\log \alpha_1 - \log \alpha_2)/(\delta_2 - \delta_1) = \log f/f_{\text{modal}}.$$

The latter equation means that the slope of the regression of $\delta_i$ on $\log f/f_{\text{modal}\,i}$, when inverted and multiplied by $-1$, gives a quantity whose antilogarithm is the magnitude of the value of $f/f_{\text{modal}}$ at which the functions intersect (Stevens, 1974; Stevens & Rubin, 1970). When the equation is applied to psychophysical data, the estimated value of the independent variable can sometimes be interpreted meaningfully. For example, it may be the value of a strong stimulus that approximates the pain threshold and indexes a ceiling level for the modality (Stevens, 1974). Applying the equation to the power spectral data of the present experiments revealed an intersection value of $f/f_{\text{modal}} = 0.016$, with 95% confidence limits of .03 and .006. Given that $f_{\text{modal}}$ was in the vicinity of 1 Hz (mean period was 1.117 s, range was 0.604–1.736 s), the preceding values can be taken as approximations to an actual frequency value and its range. The question arises: If this value is reliable, to what does it refer?

Our conjecture to be pursued is that the obtained value identifies the limit cycle regulation of oxygen consumption. Because oxygen is the only major substance essential to metabolism for which there is little or no storage, the choking of oxygen emerges as the effective regulator of muscle action (Bloch & Iberall, 1982; Iberall, 1974). That is, the level of operation of local muscle engines is regulated by an oxygen choke that limits the oxygen supply and thus the rate of local oxidation. This appears to be achieved in a 30–120 s cycle of capillary red blood flow, mediated by the vasodilatory effect of adrenaline (Iberall, 1974). A cycle of 0.01 Hz (or thereabouts) is the idling metabolic rate—the metabolic power averaged over the entire organism fluctuates at this frequency (Iberall, 1969; Iberall & Cardon, 1964), which is a plausible approximation of the time over which oxygen balance will occur within the muscular microstructure. The 30–120 s range for this proposed limit cycle is consistent with the understanding that biological cycles (fractal rhythms) are not individually stationary but wander over a stationary, stochastic distribution; that is, the spectral lines warble rather than exhibit a single fixed frequency (Bloch et al., 1971).

Table 2
*Range, Mean, and Standard Deviation of $\delta$ and $\alpha$ for Each Subject*

| | $\delta$ | | | $\alpha$ | | |
|---|---|---|---|---|---|---|
| Subject | min | max | $M \pm SD$ | min | max | $M \pm SD$ |
| 1 | 2.02 | 2.41 | 2.74 ± 0.20 | 6.17 | 20.89 | 6.17 ± 1.66 |
| 2 | 1.64 | 2.94 | 2.52 ± 0.32 | 1.17 | 16.60 | 3.47 ± 2.09 |
| 3 | 2.09 | 2.96 | 2.62 ± 0.19 | 1.66 | 19.95 | 4.37 ± 1.95 |

## General Discussion

Ostensibly, tapping the same rhythm with foot and finger simultaneously is a relatively simple everyday achievement. But what does it entail? Figure 5 shows that there is considerable moment-to-moment adjustment in the phase relation between two rhythmic units attempting to beat to the same tempo. The complexity of the time series of relative phase suggests that achieving 1:1 frequency locking of two or more limbs, or absolute coordination as von Holst (1939/1973) described it, is an active process, possibly involving rhythmicities at a number of levels. In many respects, a hypothesis that interlimb coordination is a consequence of many unseen layers of processes is not especially clever. By definition, biological movement involves many active components at many length scales—from the highly visible joint changes to the difficult-to-observe changes in myofibrils, vascular beds, and their respective molecular microstructures. What makes the hypothesis nontrivial, however, is that these heterogeneous components are subsystems of a more macroscopic, unitary organization that is sustained through nonlinear couplings (Iberall, 1978). The unitary nature of the resulting organization is exhibited in the regularity with which the patterning

of an order parameter (such as relative phase) is manipulated by some change in the state of the system (e.g., the parameterization of Ω).

From ideas underlying the dynamics of the circle map, taken here as an example of the archetypal method that nature uses to establish 1:1 frequency lockings, it was expected that where interlimb coordination satisfies $W = 1{:}1$, and the ratio of uncoupled frequencies Ω is variable, the power spectrum of relative phase should be affected in particular ways by the deviation of Ω from 1. Namely, it was predicted that the spectrum should reveal an increase in total power. Furthermore, from the related ideas underlying the theories of homeokinetics and fractal time, it was expected that because the system being investigated is a complex one involving many layers of space–time organization, the increasing total power would be redistributed across the time scales in ways specific to maintaining stability. This redistribution would result in local and global changes in the shape of the power spectrum. What was observed was an increase in the total power as a function of Ω that represented a concentration of the power at spectral peaks that were integer multiples of the coordinated frequency of oscillation of the frequency-locked wrist–pendulum systems. Old spectral peaks grew in magnitude and new peaks at higher integer multiples were added as Ω increased. Furthermore, the spectrum of the relative phase changed not only locally in the form of spectral peaks but also changed globally in the way the total power was distributed across the entire spectrum. The spectra exhibited a flattening of inverse power-law behavior given by the term $1/f^{\delta}$. These results leave a number of questions, to which only tentative answers can be provided here.

### *Why Are Spectral Peaks Integer Multiples of the Frequency of Oscillation?*

A harmonic organization of a complex system that contains a number of cyclic subcomponents is a universal strategy for providing a unitary integration of a number of components. Systems that have components operating at frequencies that are integer multiples have their cyclicities nested such that they can begin cycles at the same points in time. Hence, control of all components can be relegated to specific, discrete control points in the cycle. Such control points in perceiving–acting systems have been referred to as *organizing centers* or *intentional attractors*. For example, in the skill of juggling, these discrete control centers occur at the launch and interception of the ball by the hands (Beek, 1989). There is some evidence that in rhythmic finger movements the points of maximal excursion are the anchor points of coordination (as can be observed from a phase plane representation of this activity by Kay 1988, p. 351, Figure 4, in which the discrete nature of the turning point is clearly visible). Similarly, in wrist–pendulum swinging, the points of maximal excursion seem to be the organizing centers of control in that the dynamics associated with the radial flexion and extension switch at these locations. The integer multiple nature of the spectral peaks may be a consequence of this kind of intracycle organization. However, empirical evidence of the phasing of the involved components is necessary to validate this claim.

### *What Underlying Processes Do the Spectral Peaks Represent?*

Are they divisible into functionally different physiological (muscular, vascular, neuronal, etc.) processes? The even multiples of the coordinative frequency may index a partitioning of the flexion–extension activity at the wrist joint. It is harder to understand how the odd multiples would take part in this partitioning. No matter what their particular instantiation, it can be argued that the spectral peaks represent "energy release" mechanisms of the control structure (coordinative structure) assembled to produce 1:1 frequency locking. As such, they would function to maintain coherently the stability of the phasing under inherently unstable parameterizations. They would represent the heretofore unobserved way a coordinative structure maintains the equifinality of its task goal. In this case, the equifinal conditions of 1:1 frequency locking would be established by coherently packaging the ensuing variability.

### *Why Are the Spectral Peaks Added at Higher Frequencies as the System Becomes More Unstable?*

This strategy of adding spectral peaks is a temporal analog to the size principle that underlies motoneuron recruitment: As more and more force is used at a joint, larger motoneurons are recruited first, followed by smaller and smaller motoneurons. In the present case, cyclical processes at smaller and smaller time scales are used as the frequency-locking situation becomes less and less stable. Perhaps this is a more universal strategy used by biological systems in marshaling components of their microstructures. The introduction of peaks at higher frequencies probably reflects the general tendency of the system to scale power to $1/f^{\delta}$. The multiple regression analyses of $\log f/f_{\text{modal}}$ and $|\log \Omega|$ on the log power exhibited at the integer multiples yields a $\delta$ of around 2.5 for the scaling of the power at the integer spectral peaks. This value for $\delta$ reflects the scaling of the entire spectra and indeed may be its cause. Given this $1/f^{\delta}$ scaling and an increase in the power at the peaks as Ω increases, new peaks at higher frequencies can be expected.[3]

### *Why Is the Circle Map Prediction of Increasing Total Power With Deviation of Ω From 1 Confirmed Only for the Range $\Omega \leq 1$?*

For the values of $\Omega \geq 1$, there is no significant change of total power with Ω. Why this asymmetry occurs is peculiar. The lack of increase of total power with Ω for the $\Omega \geq 1$ range may represent the fact that there were too few observations

[3] An alternative explanation of the evolution of spectral peaks at higher frequency multiples can be made if one considers that nonlinear components of limit cycle dynamics produce harmonic frequencies above the fundamental frequency. In this case, the spectral subcomponents that emerge with changes in Ω could index the muscular engine processes that underlie the changes in the nonlinear limit cycle components.

in the range of $\Omega \geq 1$ (53 of 162). Alternatively, it may reflect an asymmetry between the hands in wrist–pendulum swinging. The values of $\Omega \leq 1$ are for wrist–pendulum system combinations where the left system has a larger length than the right. Because the uncoupled frequency of oscillation is lower for systems of longer lengths, the comfortable achievement of 1:1 frequency locking results in the left system oscillating faster than its uncoupled frequency and the right system oscillating slower than its uncoupled frequency. The values of $\Omega \geq 1$ are for wrist–pendulum system combinations where the opposite is true: The right system has the longer length and the lower uncoupled frequency of oscillation. Hence in these conditions, comfortable 1:1 frequency locking results in the right system increasing its frequency and the left system decreasing its frequency. One reading of these outcomes, with possible implications for understanding the role of biological asymmetries, is that the relative phasing becomes unstable as a function of $\Omega$ only when the exigencies of 1:1 frequency locking cause the right system to oscillate slower than its uncoupled frequency.

### *What Is the Role of the Nonspecific Subtask at Approximately 0.01 Hz?*

The conjecture that the ideal intersection of the 162 logarithmic power spectra functions is the frequency of the oxygen choke implies, perhaps, that all of the observed conditions of absolute coordination shared a common, large-scale, metabolic process. One interpretation of the data is that the task of interlimb 1:1 frequency locking engages a number of task-specific subtasks that will be partially or fully recruited depending on $\Omega$ and that will vary in the overall power required to execute them, also dependent on $\Omega$. Additionally, there are nonspecific subtasks, that is, subtasks that must be conducted regardless of the particular focal task (here, absolute interlimb coordination). Prominent among these is the blood flow process at approximately 0.01 Hz to provide the fuel, oxygen, and hormones to sustain whatever activity is being performed (Bloch et al., 1971; Bloch & Iberall, 1982). This nonspecific subtask is a design feature of the mammalian biological movement system. Its apparent manifestation in the present data is consistent with a central thesis of the homeokinetic view that a family of faster cyclicities will be stabilized and made to cohere by a slower limit cycle, particularly one that has to do with fundamental energy transactions within the system (Iberall, 1977, 1978).

### *Conclusion*

Previous studies of 1:1 frequency locking in the coordination of wrist–pendulum systems have investigated the dynamical control processes underlying the mean characteristics of the resultant kinematics, for example, mean frequency (Kugler & Turvey, 1987; Turvey et al., 1986; Turvey et al., 1988), mean amplitude (Kugler & Turvey, 1987; Kugler et al., 1990), mean relative phase (Rosenblum & Turvey, 1989; Turvey et al., 1986), the mean elastic potential of the musculature involved (Bingham et al., 1991), and the mean fluctuations of these quantities (Rosenblum & Turvey, 1989; Turvey et al., 1986; Turvey et al., 1989). Through the use of the tool of spectral analysis, a tool that has previously been used to investigate processes of motor control with great success (Beek, 1989; van Galen, van Doorn, & Schomaker, 1990; Powell & Dzendolet, 1984), the present article furthers the investigation of the dynamical control processes involved in 1:1 frequency locking by studying the relative motion of the oscillating limbs as found in the continuous relative phase time series. The results reveal that structure is latent in the variability of the relative motions and can be interpreted as indexing subprocesses that underlie 1:1 frequency locking. These results encourage further experimental explorations, using spectroscopic concepts and methods, of the rich dynamical substructure of coordinated movement patterns. Given the many subsidiary processes that provide a foundation for human action, the study of integrated activity rests on the development of concepts and methods by which the assembling of coordinated movement patterns is understandable as the establishment of relations within and across macro and micro space–time scales (Kugler & Turvey, 1987; Schöner & Kelso, 1988; Turvey, 1990).

## References


Abraham, R. H., & Shaw, C. D. (1982). *Dynamics—The geometry of behavior: Part 1. Periodic behavior.* Santa Cruz, CA: Ariel Press.

Aggashyan, R. V., Gurfinkel, V. S., & Fomin, S. V. (1973). Correlation and spectral analysis of the fluctuations of the human body during standing. *Biophysics, 18,* 1105–1108.

Arnold, V. I. (1965). Small denominators: I. Mappings of the circumference onto itself. *Transactions of The American Mathematical Society, 2nd Series, 46,* 213–284.

Arnold, V. I. (1983). *Geometrical methods in the theory of ordinary differential equations.* New York: Springer-Verlag.

Beek, P. J. (1989). *Juggling dynamics.* Amsterdam: Free University Press.

Bingham, G. P., Schmidt, R. C., Turvey, M. T., & Rosenblum, L. D. (1991). Task dynamics and resource dynamics in the assembly of a coordinated rhythmic activity. *Journal of Experimental Psychology: Human Perception and Performance, 17,* 359–381.

Bloch, E. S., Cardon, S., Iberall, A., Jacobowitz, D., Kornacker, K., Lipetz, L., McCulloch, W., Urquhart, J., Weinberg, M., & Yates, F. (1971). *Introduction to a biological systems science* (NASA CR-1720). Springfield, VA: National Technical Information Service.

Bloch, E. S., & Iberall, A. S. (1982). Toward a concept of the functional unit of mammalian skeletal muscle. *American Journal of Physiology, 242,* R411–R420.

Feder, J. (1988). *Fractals.* New York: Plenum Press.

Fein, A. P., Heutmaker, M. S., & Gollub, J. P. (1985). Scaling at the transition from quasiperiodicity to chaos in a hydrodynamic system. *Physica Scripta, T9,* 79.

Goldberger, A. L., Bhargava, V., West, B. J., & Mandell, A. J. (1985). On a mechanism of cardiac electrical stability: The fractal hypothesis. *Biophysics Journal, 48,* 525–528.

Goldberger, A. L., Kobalter, K., & Bhargava, V. (1986). $1/f$-like scaling in neutrophil dynamics: Implications for hematologic monitoring. *IEEE Transactions on Biomedical Engineering, 33,* 874–876.

Haken, H., Kelso, J. A. S., & Bunz, H. (1985). A theoretical model of phase transitions in human hand movements. *Biological Cybernetics, 51,* 347–356.

Haken, H., & Wunderlin, A. (1990). Synergetics and its paradigm of self-organization in biological systems. In H. T. A. Whiting, O. G. Meijer, & P. C. W. van Wieringen (Eds.), *The natural-physical approach to movement control* (pp. 1–36). Amsterdam: VU University Press.

Haucke, H., & Ecke, R. (1987). Mode-locking and chaos in Rayleigh-Benard convection. *Physica, 25D,* 307–329.

Iberall, A. S. (1969). A personal overview, and new thoughts in biocontrol. In C. Waddington (Ed.), *Towards a theoretical biology: 2. Sketches* (pp. 166–178). Chicago: Aldine.

Iberall, A. S. (1974). *Bridges in science: From physics to social science.* Upper Darby, PA: General Technical Services.

Iberall, A. S. (1977). A field and circuit thermodynamics for integrative physiology: I. Introduction to the general notions. *American Journal of Physiology, 233,* R171–R180.

Iberall, A. S. (1978). A field and circuit thermodynamics for integrative physiology: III. Keeping the books—A general experimental method. *American Journal of Physiology, 234,* R85–R97.

Iberall, A. S., & Cardon, S. (1964). Control in biological systems—A physical review. *Annals of The New York Academy of Sciences, 117,* 445–518.

Iberall, A. S., Soodak, H., & Hassler, F. (1978). A field circuit thermodynamics for integrative physiology: II. Power and communicational spectroscopy in biology. *American Journal of Physiology, 234,* R3–R19.

Jackson, E. A. (1989). *Perspectives of nonlinear dynamics.* Cambridge, England: Cambridge University Press.

Jensen, M. H., Bak, P., & Bohr, T. (1984). Transition to chaos by interaction of resonances in dissipative systems: I. Circle maps. *Physical Review A, 30,* 1960–1969.

Kay, B. A. (1988). The dimensionality of movement trajectories and the degrees of freedom problem: A tutorial. *Human Movement Science, 7,* 343–364.

Kelso, J. A. S. (1984). Phase transitions and critical behavior in human bimanual coordination. *American Journal of Physiology, 246,* R1000–R1004.

Kelso, J. A. S., & Scholz, J. P. (1985). Cooperative phenomena in biological motion. In H. Haken (Ed.), *Complex systems: Operational approaches in neurobiology, physical systems, and computers* (pp. 124–149). Berlin: Springer-Verlag.

Koboyashi, M., & Musha, T. (1982). $1/f$ fluctuation of heartbeat period. *IEEE Transaction on Biomedical Engineering, 29,* 456–457.

Kugler, P. N., & Turvey, M. T. (1987). *Information, natural law, and the self-assembly of rhythmic movement.* Hillsdale, NJ: Erlbaum.

Kugler, P. N., Turvey, M. T., Schmidt, R. C., & Rosenblum, L. D. (1990). Investigating a nonconservative invariant of motion in coordinated rhythmic movements. *Ecological Psychology, 2,* 151–189.

Musha, T., Katsurai, K., & Teramachi, Y. (1985). Fluctuation of human tapping intervals. *IEEE Transactions on Biomedical Engineering, 32,* 578–581.

Powell, G. M., & Dzendolet, E. (1984). Power spectral density analysis of lateral human standing sway. *Journal of Motor Behavior, 16,* 424–441.

Press, W. H., Flannery, B. P., Teukolsky, S. A., & Vetterling, W. T. (1988). *Numerical recipes in C: The art of scientific computing.* Cambridge, England: Cambridge University Press.

Rosenblum, L. D., & Turvey, M. T. (1988). Maintenance tendency in coordinated rhythmic movements: Relative fluctuations and phase. *Neuroscience, 27,* 289–300.

Schmidt, R. C., Carello, C., & Turvey, M. T. (1990). Phase transitions and critical fluctuations in the visual coordination of rhythmic movements between people. *Journal of Experimental Psychology: Human Perception and Performance, 16,* 227–247.

Schöner, G., & Kelso, J. A. S. (1988). Dynamic pattern generation in behavioral and neural systems. *Science, 239,* 1513–1520.

Schuster, H. G. (1988). *Deterministic chaos.* Weinheim, Federal Republic of Germany: VCH.

Shlesinger, M. F. (1987). Fractal time and $1/f$ noise in complex systems. *Annals of the New York Academy of Sciences, 504,* 214–228.

Stavans, J. (1987). Experimental study of quasiperiodicity in a hydrodynamical system. *Physical Review A, 35,* 4314–4328.

Stevens, J. C. (1974). Families of converging power functions. In H. R. Moskowitz et al. (Eds.), *Sensations and measurements* (pp. 157–165). Dordrecht, The Netherlands: D. Reidel.

Stevens, J. C., & Rubin, L. L. (1970). Psychophysical scales of heaviness and the size–weight illusion. *Perception & Psychophysics, 8,* 225–230.

Thompson, J. M. T., & Stewart, H. B. (1986). *Nonlinear dynamics and chaos.* Chichester, England: Wiley.

Turvey, M. T. (1990). Coordination. *American Psychologist, 45,* 938–953.

Turvey, M. T., Rosenblum, L. D., Schmidt, R. C., & Kugler, P. N. (1986). Fluctuations and phase symmetry in coordinated rhythmic movements. *Journal of Experimental Psychology: Human Perception and Performance, 12,* 564–583.

Turvey, M. T., Schmidt, R. C., & Rosenblum, L. D. (1989). "Clock" and "motor" components in absolute coordination of rhythmic movements. *Neuroscience, 33,* 1–10.

Turvey, M. T., Schmidt, R. C., Rosenblum, L. D., & Kugler, P. N. (1988). On the time allometry of coordinated rhythmic movements. *Journal of Theoretical Biology, 130,* 285–325.

van Galen, G. P., van Doorn, R. R. A., & Schomaker, L. R. B. (1990). Effects of motor programming on the power spectral density function of finger and wrist movements. *Journal of Experimental Psychology: Human Perception and Performance, 16,* 755–765.

von Holst, E. (1973). *The behavioral physiology of animal and man.* Coral Gables, FL: University of Miami Press. (Original work published 1939)

West, B. J. (1988). Fractal models in physiology. In J. A. S. Kelso, A. J. Mandell, & M. F. Shlesinger (Eds.), *Dynamic patterns in complex systems* (pp. 236–247). Singapore: World Scientific.

West, B. J., & Goldberger, A. L. (1987). Physiology in fractal dimensions. *American Scientist, 75,* 354–365.

West, B. J., & Shlesinger, M. F. (1989). On the ubiquity of $1/f$ noise. *International Journal of Modern Physics, B, 3,* 795–819.

West, B. J., & Shlesinger, M. F. (1990). The noise in natural phenomena. *American Scientist, 78,* 40–45.

Received July 13, 1990
Revision received January 7, 1991
Accepted October 23, 1990 ■